JOURNAL OF BACTERIOLOGY, Aug. 2011, p. 3912–3922 Vol. 193, No. 15
0021-9193/11/$12.00 doi:10.1128/JB.00386-11

The Riboswitch Regulates a Thiamine Pyrophosphate ABC Transporter of the Oral Spirochete *Treponema denticola*▽†

Jiang Bian,[1] Hongwu Shen,[2] Youbin Tu,[3] Aiming Yu,[2] and Chunhao Li[1]*

Department of Oral Biology, The State University of New York at Buffalo, Buffalo, New York 14214[1]; Department of Pharmaceutical Sciences, The State University of New York at Buffalo, Buffalo, New York 14260[2]; and Department of Bioinformatics, Soochow University, Suzhou 215123, China[3]

Received 22 March 2011/Accepted 13 May 2011

Thiamine pyrophosphate (TPP), a biologically active form of thiamine (vitamin B_1), is an essential cofactor in all living systems. Microorganisms either synthesize TPP via *de novo* biosynthesis pathways or uptake exogenous thiamine from the environment via specific transporters. The oral spirochete *Treponema denticola* is an important pathogen that is associated with human periodontal diseases. It lacks a *de novo* TPP biosynthesis pathway and needs exogenous TPP for growth, suggesting that it may obtain exogenous TPP via a thiamine transporter. In this study, we identified a gene cluster that encodes a TPP ABC transporter which consists of a TPP-binding protein (TDE0143), a transmembrane permease (TDE0144), and a cytosolic ATPase (TDE0145). Transcriptional and translational analyses showed that the genes encoding these three proteins are cotranscribed and form an operon (*tbpABC*$_{Td}$) that is initiated by a σ^{70}-like promoter. The expression level of this operon is negatively regulated by exogenous TPP and is mediated by a TPP-sensing riboswitch (Td$_{thi\text{-box}}$). Genetic and biochemical studies revealed that the *TDE0143* deletion mutant (*T. denticola* Δ*tbpA*) had a decreased ability to transport exogenous TPP, and the mutant failed to grow when exogenous TPP was insufficient. These results taken together indicate that the *tbpABC*$_{Td}$ operon encodes an ABC transporter that is required for the uptake of exogenous TPP and that the expression of this operon is regulated by a TPP-binding riboswitch via a feedback inhibition mechanism.

Human periodontal diseases are a group of infections that affect the structures surrounding teeth and occur in 80% of the adult population at some time in their lives (59, 72, 75). The diseases are caused primarily by polymicrobial infections followed by host factors (13). In the oral cavity, more than 700 different microorganisms have been identified (17, 41, 56), and they typically live in a synergetic manner (28, 72). In the symbiotic mode, the existence of one group of bacteria may create a nutritional and atmospheric environment that can facilitate the colonization and growth of other microorganisms (e.g., the metabolites from one group of bacteria can be used as an energy source by others). Thus, studying bacterial metabolism can help us to understand the ecology of these oral microorganisms and the etiology of periodontal diseases.

In the oral microflora there is a substantial amount of spirochetes, and more than 60 different species have been identified. 16S rRNA gene sequence analyses indicate that all of these oral spirochetes belong to one genus, *Treponema* (17, 56). However, due to their fastidious growth requirements and the lack of understanding of their nutritional metabolism, very few oral treponemes have been cultivated (8, 20). *Treponema denticola* is an oral spirochete that can be easily cultivated. Since its genome was sequenced and it can be genetically manipulated, *T. denticola* has been used as a model spirochete to study other oral spirochetes (20, 39, 44, 85). *T. denticola* is a member of the "red-complex" bacteria, which are a group of Gram-negative, anaerobic, and proteolytic oral bacteria that are highly associated with human periodontal diseases (13, 30). A group of studies have shown that *T. denticola* is associated with the incidence and severity of periodontal diseases, and several virulence-associated factors have been characterized (14, 20, 21, 46, 67).

T. denticola is a motile, fastidious, and obligate anaerobic bacterium that dwells in a complex and diverse microbial community within the oral cavity (29, 64). In order to survive in this highly specialized milieu and cause diseases, *T. denticola* has to acquire essential nutrients, overcome the competition with other bacterial species, and protect against the constant pressure of host defenses. Previous studies have focused on its genetics and pathogenesis, and very few studies have investigated the metabolism of *T. denticola* (4, 7, 12, 22, 29, 31, 35, 63). As an obligate bacterium, *T. denticola* needs exogenous fatty acids, amino acids, and vitamins to grow (4, 29). Among these nutrients, thiamine pyrophosphate (TPP), an active form of thiamine, is an essential cofactor of several important enzymes in carbohydrate and branched-chain amino acid metabolism, and it is needed by all living organisms (2, 18, 36, 62). In addition, thiamine biosynthesis (TBS) is often linked to other central metabolic pathways such as purine biosynthesis (2, 18, 36). Thus, studying the thiamine biosynthesis of a microorganism can help us to dissect its metabolic integration.

Bacteria either produce TPP via a *de novo* biosynthesis pathway or uptake exogenous TPP from the environment (2, 34). *T. denticola* needs exogenous TPP to support its growth (16), and yet neither *de novo* nor salvage TPP synthesis pathways have been identified, suggesting that *T. denticola* may uptake exogenous TPP via a specific transport system (70). In *Salmo-*

* Corresponding author. Mailing address: Department of Oral Biology, SUNY at Buffalo, 3435 Main St., Buffalo, NY 14214-3902. Phone: (716) 829-6014. Fax: (716) 829-3942. E-mail: cli9@buffalo.edu.

† Supplemental material for this article may be found at http://jb.asm.org/.

▽ Published ahead of print on 27 May 2011.

nella enterica serovar Typhimurium, the *thiBPQ* operon encodes a TPP ABC transporter that consists of a thiamine-binding protein (ThiB), a transmembrane thiamine channel (ThiP), and an ATPase (ThiQ) (80). Genetic studies have shown that this transporter is required for the uptake of exogenous TPP, and it is essential for the growth of *S.* Typhimurium that has its *de novo* biosynthesis pathway disrupted (80). In this study, an operon that encodes a putative TPP ABC transporter was identified in *T. denticola*. Genetic and biochemical studies showed that this transporter is involved in the uptake of exogenous TPP, and it is essential for growth of *T. denticola* when the exogenous TPP is limited.

The riboswitch is a common regulatory mechanism that is often involved in the biosynthesis of amino acids, nucleotides, vitamins, and other molecules, and it has been identified in many organisms, including bacteria, archaea, fungi, and plants (5, 53, 60, 68, 83). Riboswitches are structured domains that usually reside in the noncoding regions of mRNAs (52, 68), where they bind metabolites and control gene expression. Each class of riboswitches identified so far forms a structured receptor, or "aptamer," that directly binds to a specific metabolite (19, 69, 83). In *Escherichia coli* and *S.* Typhimurium, three thiamine biosynthetic operons (*thiCEFSGH*, *thiMD*, and *thiBPQ*) are negatively regulated by TPP and are mediated by the thiamine-sensing riboswitch (*thi*-box) (51, 69, 82). It has been experimentally demonstrated that the *thi*-box of *thiM* regulates the *thiMD* operon at the translational level by sequestering the Shine-Dalgarno (S/D) sequence. This prevents the ribosome from binding to the mRNA and translating the transcript (54, 82). The regulatory mechanism of *thiC* remains elusive. It has been postulated that the *thi*-box of *thiC* controls the *thiCEFSGH* operon by premature transcription termination (5, 82). In this study, it was found that the expression of the identified TPP transporter of *T. denticola* was regulated at the transcriptional level by a *thi*-box.

MATERIALS AND METHODS

Bacterial strains and growth conditions. *T. denticola* ATCC 35405 (wild type) (70) and the isogenic mutant described below were grown in OBGM medium with 10% heat-inactivated rabbit serum (55) at 37°C in an AS-580 anaerobic chamber (Anaerobe Systems, Morgan Hill, CA) with an atmosphere of 85% nitrogen, 5% carbon dioxide, and 10% hydrogen. For the semisolid medium, 0.7% low-melting-point SeaPlaque agarose (Lonza, Rockland, ME) was incorporated into the medium, and the plates were poured after inoculating a bacterial suspension into the medium at 37°C (44, 45). *Escherichia coli* strain TOP10 (Invitrogen, Carlsbad, CA) was used for DNA cloning and β-galactosidase assays, and the BL21 Codon Plus strain (Stratagene, La Jolla, CA) was used for preparing the recombinant protein. The *E. coli* strains were cultured in lysogeny broth (LB) supplemented with appropriate concentrations of antibiotics.

Preparation of TA medium. To prepare a medium with a defined amount of TPP, the concentration of TPP in the OBGM medium was detected by high-performance liquid chromatography (HPLC) as described below. The concentrations of TPP in the OBGM medium, with and without additional TPP, were 14 μM and 1 μM, respectively. Analysis showed that brain heart infusion (BHI) and yeast extract are the main sources of TPP. To reduce the level of TPP in the medium, the amounts of BHI and yeast extract in the OBGM medium were decreased to 2.5 g liter^{-1} and 1.5 g liter^{-1}, respectively, which reduced the concentration of TPP to approximately 100 nM. The rest of the components in the medium are the same as in the normal OBGM medium. The obtained medium was referred to as TPP assay (TA) medium. In this study, media containing three different concentrations of TPP (100 nM, 10 μM, and 50 μM) were prepared.

Detection of TPP by HPLC. The TPP concentrations in the media and in the *T. denticola* cells were measured by high-performance liquid chromatography (HPLC) as previously described (37, 47) with some modifications. To detect intracellular TPP, 50 ml of stationary-phase *T. denticola* culture, which was cultivated in the TA media with three different concentrations of TPP, was harvested by centrifugation at 6,000 × *g* for 10 min. The resulting cell pellets were washed twice with phosphate-buffered saline (pH 7.4) (PBS) and then resuspended in PBS. The final cell densities were adjusted to approximately 10^{10} cells ml^{-1}. The obtained samples were lysed with a French press and fractionated by centrifugation at 10,000 × *g* for 10 min. The resulting supernatants were first precipitated with a 3-fold volume of methanol and then centrifuged at 16,000 × *g* for 10 min. After the centrifugation, 100 μl of the supernatant was treated with a freshly prepared derivatization buffer (0.2 mM potassium ferricyanide and 5% sodium hydroxide) to oxidize TPP to the thiochrome derivative that can be fluorimetrically detected by HPLC. Five microliters of the obtained samples was processed for HPLC analysis.

Quantification of TPP was performed on an Agilent (Palo Alto, CA) 1100 series HPLC system consisting of an online vacuum degasser, quaternary pump, autosampler, thermostat-controlled column compartment, and fluorescence detector. Sample separation was achieved using a Phenomenex (Torrance, CA) Luna C_{18} column (100 mm by 2.0 mm by 3 μm). A gradient elution was employed to separate the samples. The elution parameters were as follows: an initial 3-min isocratic elution with 95% buffer A (0.02% trifluoroacetic acid in water) and 5% buffer B (0.02% trifluoroacetic acid in 90% acetonitrile), a linear increase of buffer B to 40% for 2 min and then elution with 40% buffer B for 7 min, followed by the initial condition from 13 min. TPP was detected at an excitation wavelength of 375 nm and an emission wavelength of 430 nm using a fluorescence detector. The calibration linear range of TPP was 0.15 to 15 pmol on the column. Three independent assays were conducted, and the intracellular TPP concentration was expressed as nanomolar.

Construction of *tbpABC*$_{Td}$ *thi*-box–*lacZ* fusions and TPP repression β-galactosidase assays. The fragment spanning from nucleotide (nt) −366 to +69 (*thi*-box-L) of the *tbpABC*$_{Td}$ operon was PCR amplified from wild-type *T. denticola* chromosomal DNA using primer pair P_{15}/P_{16} (Table 1), generating the amplicon with engineered EcoRI and BamHI cut sites at the 5′ and 3′ ends, respectively. The resultant amplicon was first cloned into the pGEM-T-Easy vector (Promega, Madison, WI) and then released by EcoRI and BamHI digestion. The obtained DNA fragment was fused to a promoterless *lacZ* gene in the pRS414 plasmid (a gift from R. Breaker, Yale University) (71, 82), in which the 23rd (*thi*-box-L) codon of *TDE0143* resides in frame with the ninth usage codon of *lacZ*. Site-direct mutagenesis of *thi*-box-L was conducted using the QuikChange II site-directed mutagenesis kit (Stratagene) with primer pair P_{29}/P_{30}, according to the manufacturer's instructions. The mutation was confirmed by DNA sequencing (Roswell Park Cancer Institute DNA Sequencing Laboratory, Buffalo, NY), and the resultant construct was named *thi*-box-Lm.

The *thi*-box-L-*lacZ* and *thi*-box-Lm–*lacZ* fusion constructs were transformed into *E. coli* TOP10 cells. A TPP repression β-galactosidase assay was conducted as previously described (82). Briefly, the *E. coli* TOP10 cells transformed with the *lacZ* fusion plasmids were grown in M9 glucose minimal medium plus 50 μg ml^{-1} vitamin assay Casamino Acids (Difco, Becton Dickinson and Company, Sparks, MD) to the mid-exponential phase either with or without TPP (100 μM). The β-galactosidase activity was measured with the β-galactosidase enzyme assay system (Promega) in 96-well plates. All experiments were repeated at least twice in duplicate.

Reverse transcription-PCR (RT-PCR), quantitative RT-PCR (qRT-PCR), and RNA ligase-mediated rapid amplification of cDNA ends (RLM-RACE). RNA isolation was carried out as previously described (42, 65). For *T. denticola*, 100 ml of mid-log-phase cultures (~ 5 × 10^7 cells ml^{-1}) were harvested for RNA preparations; for *E. coli*, following the TPP repression β-galactosidase assays described above, 10 ml of the mid-exponential-phase cultures was harvested for RNA preparations. Total RNA was extracted using TRI reagent (Sigma-Aldrich, St. Louis, MO) according to the manufacturer's instructions. The resultant samples were treated with Turbo DNase I (Ambion, Austin, TX) at 37°C for 2 h to eliminate genomic DNA contamination. The resultant RNA samples were extracted using acid-phenol–chloroform (Ambion), precipitated in isopropanol, and washed with 70% ethanol. The RNA pellets were resuspended in RNase-free water. RNA (1 μg) was reverse transcribed using the avian myeloblastosis virus (AMV) reverse transcriptase (Promega) to generate cDNA.

For RT-PCR analysis, 1 μl of cDNA was PCR amplified using *Taq* DNA polymerase (Qiagen, Valencia, CA). The qRT-PCR analysis was conducted using iQ SYBR green Supermix and MyiQ thermal cycler (Bio-Rad, Hercules, CA), as previously described (74). The genes encoding heat shock proteins GroEL (*E. coli*) and DnaK (*T. denticola TDE0628*) were used as internal controls to normalize the qRT-PCR data. The primers used for the RT-PCR and qRT-PCR analyses are listed in Table 1. To determine the transcription start site

TABLE 1. Oligonucleotide primers used in this study

Primer	Sequence (5′ → 3′)[a]	Comment[b]
P_1	GACAGTTTACTCGGCACG	Flanking region before *TDE0143*; F
P_2	ATCGATCAGCCCTTTGCGGGTATG	Flanking region before *TDE0143*; R
P_3	ATCGATCTCAAAGCCTCCTTCCCG	Flanking region after *TDE0143*; F
P_4	AGATATTTCGGTGAGGGC	Flanking region after *TDE0143*; R
P_5	ATCGATCCGATAGCTTCCGCTATTGC	*erm* cassette; F
P_6	ATCGATGGAAGCTGTCAGTAGTATACC	*erm* cassette; R
P_7	CGGAGAAGCTCCCATAGC	Co-RT-PCR, *TDE0143-TDE0144*; F
P_8	AAAGATGAGGCCGCCGAG	Co-RT-PCR, *TDE0143-TDE0144*; R
P_9	CCCATGTGCAAGAAGGGC	Co-RT-PCR, *TDE0144-TDE0145*; F
P_{10}	GACCATTCCGATTCCGCG	Co-RT-PCR, *TDE0144-TDE0145*; R
P_{11}	CATTACCCCTCTTGTCGAG	Co-RT-PCR, *TDE0145-TDE0146*; F
P_{12}	CGTTAATCTCGGCTATACC	Co-RT-PCR, *TDE0145-TDE0146*; R
P_{13}	CACCTGTGCCGCTCTTTTTGCA	$rTbpA_{Td}$; F
P_{14}	CTAAGCAAGTCCCTTGATAAC	$rTbpA_{Td}$; R
P_{15}	GAATTCGGACAACTTGTTATTATGCAC	5′ of $tbpA_{Td}$ *thi*-box; F
P_{16}	GGATCCTGCAAAAAGAGCGGCACAACC	3′ of $tbpA_{Td}$ *thi*-box-L; R
P_{17}	GGATCCCATATGCTCCCTCCGCCGGTA	3′ of $tbpA_{Td}$ *thi*-box-S; R
P_{18}	TAATTATCGGTTGTGCCGCT	*TDE0143* 5′-RACE sensor primer; F
P_{19}	CGGCAATACCCATACCTTCA	*TDE0143* 5′-RACE inner primer; R
P_{20}	TGCAGGTTTGGGAACATCCT	*TDE0143* 5′-RACE outer primer; R
P_{21}	CTGACGGAACAAAGGTTGTAG	qRT-PCR, *TDE0143*; F
P_{22}	CCTTACCTTCCAGTATGACTC	qRT-PCR, *TDE0143*; R
P_{23}	TAGGATTGCTGCCTTTACGG	qRT-PCR, *TDE0144*; F
P_{24}	ATTATTGCAGGCACGCAGAG	qRT-PCR, *TDE0144*; R
P_{25}	TCAGGCTGCGGCAAAACAAC	qRT-PCR, *TDE0145*; F
P_{26}	CATTGAGATGAGGGAAGAGG	qRT-PCR, *TDE0145*; R
P_{27}	CCGTCCATTGTAGGCTTTAC	qRT-PCR, *dnaK*; F
P_{28}	CCGTCAATGTCGATTCGTAC	qRT-PCR, *dnaK*; R
P_{29}	TGCTTTTACAAGCTAAAAACATACCCGCAA	TPP-binding site mutagenesis; F
P_{30}	TTGCGGGTATGTTTTTAGCTTGTAAAAGCA	TPP-binding site mutagenesis; R
P_{31}	GCAGCACATCCCCCTTTC	qRT-PCR, *lacZ*; F
P_{32}	CGTTGGTGTAGATGGGCG	qRT-PCR, lacZ; R
P_{33}	AACGTACTGGCAGATGCAG	qRT-PCR, *groEL*; F
P_{34}	GCGCTTTCAGTTCTTCAACTG	qRT-PCR, *groEL*; R

[a] The engineered restriction enzyme sites are underlined.
[b] F, forward primer; R, reverse primer.

upstream of *TDE0143*, 5′-RACE analysis was carried out using the FirstChoice RLM-RACE kit (Ambion) according to the manufacturer's protocol. Purified *T. denticola* RNA (10 μg) was reverse transcribed to cDNA with a 5′-RACE adapter, followed by PCR amplifications with primers P_{18}, P_{19}, and P_{20} (Table 1). The resultant PCR products were cloned into the pGEM-T-Easy vector and sequenced (Roswell Park Cancer Institute DNA Sequencing Laboratory).

Construction of a *T. denticola tbpA*$_{Td}$ deletion mutant (*T. denticola* Δ*tbpA*). To inactivate *tbpA*$_{Td}$ (*TDE0143*), its flanking regions were PCR amplified from wild-type *T. denticola* genome DNA using the primer pairs P_1/P_2 and P_3/P_4 (Fig. 1 and Table 1). A previously described (45) *ermF/AM* erythromycin resistance cassette (Erm^r) was PCR amplified using the primer pair P_5/P_6. The amplicons were individually cloned into the pGEM-T-Easy vector (Promega). The downstream fragment (flanking R2) was released by ClaI and SphI digestion and then ligated to the 3′ end of the upstream fragment (flanking R1) at the same cut sites. The Erm^r cassette was then released by ClaI digestion and inserted into the obtained fragment described above, generating the *tbpA*$_{Td}$*::erm* plasmid, in which a 864 bp of *TDE0143* fragment was deleted (Fig. 1). For the allelic replacement mutagenesis, the *tbpA*$_{Td}$*::erm* plasmid was linearized with NotI. Approximately 10 μg of the linearized plasmid was electroporated into wild-type *T. denticola* cells, and the transformed cells were selected on semisolid OBGM plates containing erythromycin (60 μg ml^{-1}).

Measurement of the growth rates of *T. denticola*. To measure the growth curves of *T. denticola* strains, 50 μl of PBS-washed *T. denticola* cells (3×10^8 cells ml^{-1}) were inoculated into 5 ml of TA medium (the initial cell density was 3×10^6 cells ml^{-1}) containing different concentrations of TPP (100 nM, 10 μM, and 50 μM) and incubated at 37°C in an anaerobic chamber. The cultures were enumerated every 24 h using a Petroff-Hausser counting chamber (Hausser Scientific, Horsham, PA) for up to 7 days. Counts were repeated in triplicate with at least three independent samples. The results were expressed as mean cell numbers ± standard error of the mean (SEM).

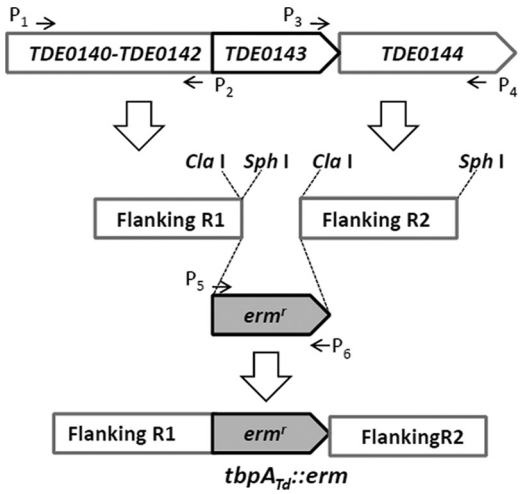

FIG. 1. Diagram showing the targeted mutagenesis of the *tbpA*$_{Td}$ gene. Arrows indicate the relative positions of PCR primers for constructing the targeted mutagenesis vector *tbpA*$_{Td}$*::erm*, in which an 864-bp *TDE0143* fragment is deleted and replaced by the erythromycin resistance cassette (Erm^r). The sequences of these primers are listed in Table 1.

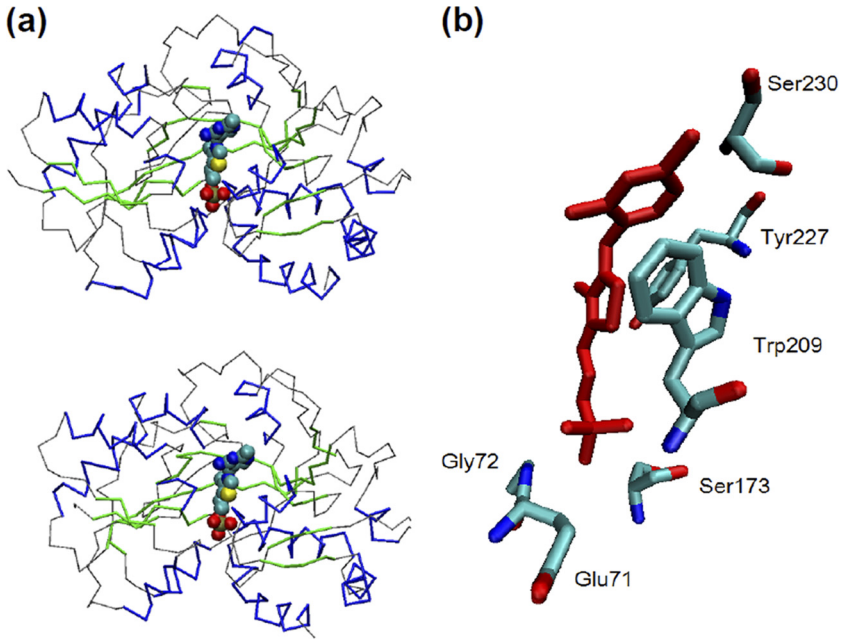

FIG. 2. Structural characteristics of $TbpA_{Td}$. (a) Comparison of the overall structures of the *E. coli* TbpA protein (top) and $TbpA_{Td}$ (bottom). The structural view of these two proteins is depicted by Cα trace with helices colored in blue, sheets in green, and the rest in gray. The TPP ligand is shown in a Van der Waals (VDW) representation. *E. coli* TbpA (Protein Data Bank ID 2QRY) (73) was selected for the structural modeling using the program Modeler 9v7 as previously described (66). (b) Predicted thiamine-binding site with the amino acids and the bound TPP (red).

Generation of $TbpA_{Td}$ antiserum. A DNA fragment that encodes the N-terminal 283 amino acids of $TbpA_{Td}$ was PCR amplified using the primers P_{13}/P_{14} (Table 1) and Platinum *Pfx* DNA polymerase (Invitrogen). The amplicon was cloned into the pET100/D-TOPO expression vector (Invitrogen), which generates a six-histidine tag at the N terminus of the recombinant protein. The resulting plasmid was then transformed into BL21 Codon Plus cells (Stratagene). The expression of recombinant $TbpA_{Td}$ ($rTbpA_{Td}$) was induced using 0.1 M isopropyl-β-D-thiogalactoside (IPTG). The recombinant protein was purified at 4°C using HisTrap HP columns (GE Healthcare, Piscataway, NJ) under denaturing conditions. The final purified protein was dialyzed in buffer (0.01 M Tris base, pH 8.0) at 4°C overnight. To produce an antiserum against $TbpA_{Td}$, mice were immunized with 1 mg of $rTbpA_{Td}$ in three inoculations during a 1-month period, and the obtained antiserum was tested with immunoblots as previously described (43).

Electrophoresis and Western blotting. Sodium dodecyl sulfate-polyacrylamide gel electrophoresis (SDS-PAGE) and Western blotting were performed as previously described (42, 43). *T. denticola* cells were harvested at approximately 10^8 cells ml^{-1} in stationary phase. The same amount of whole-cell lysates (10 to 50 μg) was separated by SDS-PAGE and then transferred to a polyvinylidene difluoride (PVDF) membrane (Bio-Rad). Immunoblots were probed with specific antibodies against $TbpA_{Td}$ or FlaA (an internal control). Immunoblots were developed using horseradish peroxidase secondary antibody with the enhanced chemiluminescent detection system (ECL). Densitometry of immunoreactive proteins in the blots was used to determine the relative amounts of proteins as previously described (74). Densitometry was done using the Molecular Imager ChemiDoc XRS imaging system (Bio-Rad).

Construction of a homology model of $TbpA_{Td}$. The crystal structure of *E. coli* TbpA protein (Protein Data Bank ID 2QRY) (73) was selected as the template for the homology modeling. Pairwise sequence alignment between $TbpA_{Td}$ and the template was conducted using Clustal X. Modeler 9v7 (66) was used to construct the homology model. Chain A of 2QRY (73) together with TPP was used as the template. The automodel class with the conjugate gradient optimization method was adopted to produce the final model with the best objective function value among the five resultant candidates. Thiamine-binding residues were picked at relative positions comparable to those in 2QRY. All diagrams were produced in VMD 1.8.7.

RESULTS

Identification of a putative TPP ABC transporter. The TPP transporter of *S.* Typhimurium consists of a thiamine-binding protein (ThiB, also named TbpA), a transmembrane thiamine channel (ThiP), and an ATPase (ThiQ, also named FbpC) (15, 33). To determine if there is any similar transporter in *T. denticola*, the genes encoding these three proteins were used as queries to search the genome of *T. denticola* strain ATCC 35405 (70). The results revealed that a gene cluster encodes a putative TPP transporter that is a homolog of ThiBPQ, in which TDE0143 has 37% identity and 54% similarity to ThiB (ZP_03051779), TDE0144 has 29% identity and 49% similarity to ThiP (YP668009), and TDE0145 has 44% identity and 69% similarity to ThiQ (ZP_05623000). These three identified proteins were further used as queries to search the Pfam database and the Conserved Domain Database (CDD) (23, 48), and the results showed that they belong to the corresponding Pfam or CDD group. For example, TDE0143 ($TbpA_{Td}$) is a member of PRK11205, a family of thiamine transporter substrate-binding subunits (see Fig. S1 in the supplemental material). Structure modeling analysis further revealed that $TbpA_{Td}$ has a structure similar to that of ThiB (Fig. 2a) and that it contains a well-conserved thiamine-binding motif (Fig. 2b), suggesting that $TbpA_{Td}$ is a thiamine-binding protein. Collectively, these results suggest that the gene cluster of *TDE0143* to *-0145* encodes a putative TPP transporter, in which *TDE0143* encodes a TPP-binding protein, *TDE0144* ($TbpB_{Td}$) encodes a transmembrane thiamine channel, and *TDE0145* ($TbpC_{Td}$) encodes an ATPase.

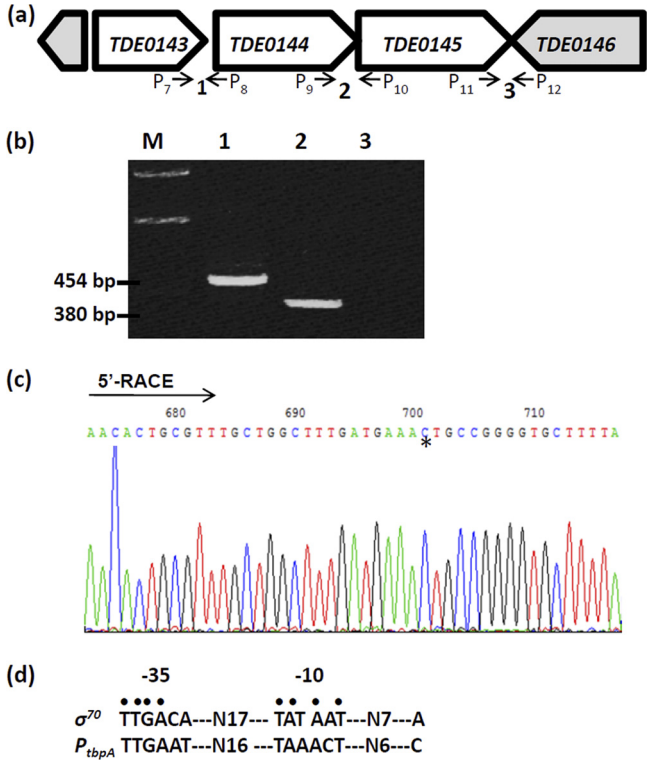

FIG. 3. Transcriptional analysis of the $tbpABC_{Td}$ operon. (a) Diagram showing the genes near *TDE0143*. The numbers and small arrows show the primers used for the RT-PCR analysis. (b) RT-PCR analysis. The lane numbers correspond to the primers labeled in panel a, and the sequences of these primers are described in Table 1. Lane M, 1.0-kb DNA ladder. (c) 5′-RLM-RACE analysis. The arrow shows the sequencing direction, and the asterisk indicates the identified transcriptional start site. (d) Comparison of the identified promoter sequence with the consensus sequence of the *E. coli* σ^{70} promoter. The conserved nucleotides are dotted.

Transcriptional analysis of the $tbpABC_{Td}$ operon. The open reading frames (ORFs) of *TDE0143*, *TDE0144*, and *TDE0145* are in the same orientation and are adjacent to each other (the maximum intergenic space is 11 bp) (Fig. 3a), suggesting that these three genes are probably cotranscribed. To confirm this speculation, RT-PCR analysis described before (84) was conducted with three pairs of primers (P_7 to P_{12} [Table 1]), spanning from *TDE0143* to *TDE0146* (Fig. 3a). As shown in Fig. 3b, the primers spanning from *TDE0143* to *TDE0145* yielded positive RT-PCR products of the predicted sizes. As expected, no product was detected between *TDE0145* and *TDE0146*, since they are divergently transcribed (Fig. 3a and b). This analysis shows that these three genes form a polycistronic operon that is transcribed as a single transcript, and this gene cluster is referred to as the $tbpABC_{Td}$ operon.

To further delineate the regulation of $tbpABC_{Td}$ operon, RLM-RACE analysis was conducted to determine its transcriptional start site. The analysis mapped the start site to the nucleotide C that is 98 nt from the start codon of *TDE0143* (Fig. 3c; see Fig. S2 in the supplemental material). A promoter-like consensus was identified at the −10 (TAAACT) and −35 (TTGAAT) regions (Fig. 3d), which is similar to those of the σ^{70} promoter of *E. coli* (26, 77), suggesting that $tbpABC_{Td}$ is probably regulated by a σ^{70}-like promoter. The identified promoter was named P_{tbpA}.

Identification of a *thi*-box at the 5′-UTR of $tbpABC_{Td}$. There is a 98-nt untranslated region (UTR) upstream of the $tbpABC_{Td}$ transcript, and a recent study projected that this region contains a putative *thi*-box (27). The predicted *thi*-box (designated $Td_{thi\text{-box}}$) is 117 nt and spans from nt −104 to +13 (counting from the start codon), which encompasses part of the P_{tbpA} promoter and the whole S/D sequence (Fig. 4a). Sequence alignment analysis further confirmed that $Td_{thi\text{-box}}$ belongs to the family of TPP riboswitches (RF00059) (27), and it contains the conserved residues involved in the binding of TPP and Mg^{2+} (19, 38, 82) (Fig. 4a). Secondary structure modeling predicted that $Td_{thi\text{-box}}$ forms a conserved TPP aptamer that consists of five helices, three terminal loops, and two junction bulges (Fig. 4b). One of these junction bulges contains the UGAGA motif that is absolutely invariant in the family of TPP riboswitches (19, 38, 82).

The expression level of the $Td_{thi\text{-box}}$–*lacZ* fusion reporter is negatively regulated by TPP. To further confirm the above proposition, TPP repression β-galactosidase assays were con-

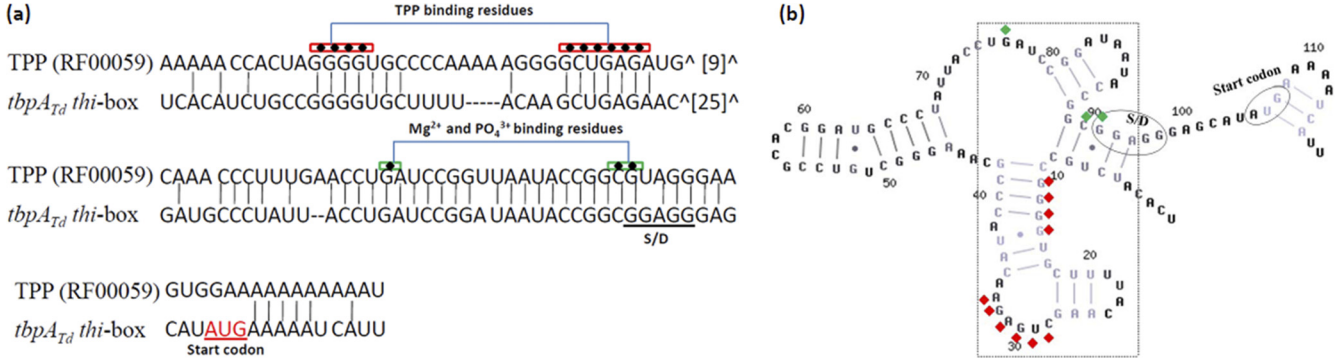

FIG. 4. Sequence and secondary structure of $Td_{thi\text{-box}}$. (a) Comparison between the 5′-untranslated region (UTR) of $tbpA_{Td}$ ($Td_{thi\text{-box}}$) and the TPP riboswitch motif box (RF00059) (27). Diamonds represent the conserved residues required for the function and structure of TPP riboswitches. The underlined AUG is the translational start codon of $tbpA_{Td}$. (b) Diamonds represent the conserved residues identified in the riboswitches of *thiM* and *thiC*. The S/D sequence and the start codon are circled. The conserved TPP-sensing motif is boxed. The structure was predicted with the CONTRAfold program.

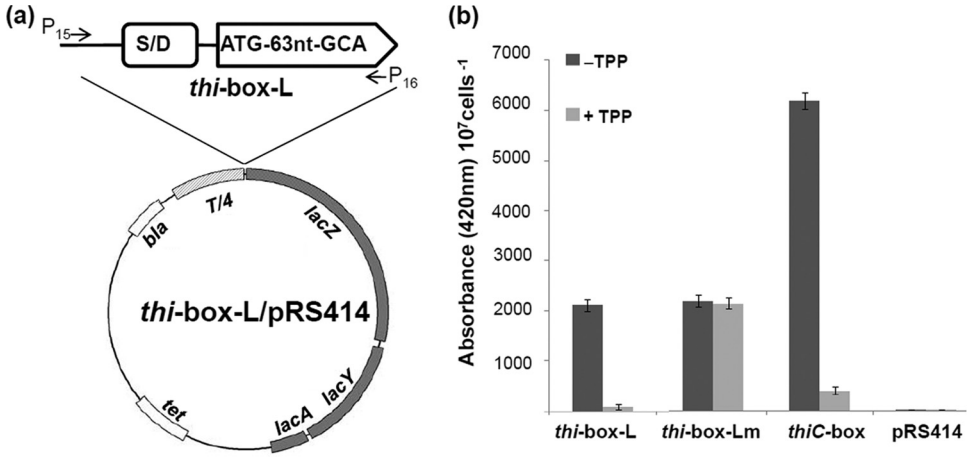

FIG. 5. Characterization of a TPP-sensing riboswitch in *T. denticola* ($Td_{thi\text{-box}}$). (a) Construction of $Td_{thi\text{-box}}$–*lacZ* fusions for the β-galactosidase assays. *thi*-box-L represents the fragment from nucleotide −366 to +69 of $Td_{thi\text{-box}}$. (b) TPP repression β-galactosidase assays. The β-galactosidase activity was expressed as Miller units/10^7 cells, and the levels represent means ± standard errors of the means from three independent experiments. Plasmid pRS414 containing the *thiC*-box was used as a positive control and plasmid pRS414 (82) as a negative control.

ducted using two $Td_{thi\text{-box}}$–*lacZ* fusion constructs (*thi*-box-L–*lacZ* and *thi*-box-Lm–*lacZ*) (Fig. 5a). The *thiC-lacZ* fusion acts as a TPP-sensing riboswitch positive control and the pRS414 plasmid as a negative control (71, 82). As expected, the β-galactosidase activity of *thiC-lacZ* was substantially reduced in the presence of TPP (100 μM), and no β-galactosidase activity was detected in the pRS414 plasmid (Fig. 5b). Similarly to that of *thiC*, the activity of *thi*-box-L--*lacZ* fusion was decreased approximately 20-fold by the addition of TPP (Fig. 5b). To determine if the reduction of β-galactosidase activity in *thi*-box-L–*lacZ* is mediated by TPP, the conserved TPP-binding site UGAGA (Fig. 4) was mutated to UAAAA in the *thi*-box-Lm–*lacZ* construct. As shown in Fig. 5b, the repression of $Td_{thi\text{-box}}$ on the β-galactosidase activity was completely abolished in the mutated construct. Collectively, these results demonstrate that $Td_{thi\text{-box}}$ is a TPP-sensing riboswitch.

The action of $Td_{thi\text{-box}}$ occurs at the transcriptional level. The action of $Td_{thi\text{-box}}$ can occur either at the translational level by preventing the ribosome from binding to the mRNA and translating the transcript or at the transcriptional level by premature transcription termination. To rule out one of these two possibilities, following the TPP repression β-galactosidase assays described above, the levels of *lacZ* mRNA were measured by qRT-PCR. As shown in Table 2, in the presence of TPP, the level of *lacZ* transcript was decreased about 16-fold (ranging from 13- to 20-fold) in the *thi*-box-L--*lacZ* construct and 13-fold (ranging from 10- to 16-fold) in the *thiC-lacZ* construct. The level of *lacZ* transcript remained unchanged in the *thi*-box-Lm–*lacZ* construct. The decreased transcript level is proportional to the results from the TPP repression β-galactosidase assays (Fig. 5), indicating that the actions of $Td_{thi\text{-box}}$ and the *thi*-box of *thiC* on the reporter gene expression occur primarily at the transcriptional level.

Expression of the *tbpABC*$_{Td}$ operon is repressed by high concentrations of TPP. To determine the effect of TPP on the expression of the *tbpABC*$_{Td}$ operon, *T. denticola* was cultured in the TPP assay (TA) medium with three different concentrations of TPP (100 nM, 10 μM, and 50 μM) as described in Materials and Methods. Among these three dosages, 10 μM TPP is similar to that in normal OBGM medium (55), 100 nM

TABLE 2. Effect of TPP on the *lacZ* transcript as evaluated by qRT-PCR analysis

E. coli sample	TPP (μM)[a]	Mean ± SEM[b]				Fold difference ($2^{-\Delta\Delta CT}$)
		C_T value		ΔC_T	$\Delta\Delta C_T$	
		lacZ	*groEL*			
thi-box-L–*lacZ*	100	17.17 ± 0.07	19.44 ± 0.09	−2.27 ± 0.09	−4.03 ± 0.29	13.36–19.97
	0	14.0 ± 0.19	20.30 ± 0.29	−6.30 ± 0.29		
thi-box-Lm–*lacZ*	100	16.61 ± 0.10	21.63 ± 0.53	−5.03 ± 0.10	−0.13 ± 0.13	1.0–1.20
	0	16.48 ± 0.10	21.64 ± 0.04	−5.16 ± 0.13		
thiC-lacZ	100	16.66 ± 0.16	21.97 ± 0.31	−5.31 ± 0.31	−3.68 ± 0.31	10.34–15.89
	0	12.83 ± 0.09	21.82 ± 0.31	−8.99 ± 0.31		
Promoterless *lacZ*	100	28.09 ± 1.58	19.28 ± 0.10	8.80 ± 1.58		
	0	26.77 ± 0.14	19.45 ± 0.13	7.33 ± 0.14		

[a] TPP added to the M9 medium for *E. coli*.
[b] C_T, threshold cycle. $\Delta\Delta C_T = \Delta C_T$ without TPP − ΔC_T with TPP.

TABLE 3. Effect of TPP on the $tbpA_{Td}$ transcript as evaluated by qRT-PCR analysis

TPP (μM)[a]	Mean ± SEM				Fold difference ($2^{-\Delta\Delta CT}$)
	C_T value		ΔC_T	$\Delta\Delta C_T$	
	$tbpA_{Td}$	*dnaK*			
50	25.00 ± 0.18	21.76 ± 0.08	3.20 ± 0.18	−4.55 ± 0.19	20.53–26.72
−	21.58 ± 0.16	22.93 ± 0.19	−1.35 ± 0.19		
10	22.35 ± 0.17	19.69 ± 0.28	2.66 ± 0.28	−4.01 ± 0.28	13.27–19.56
−	21.58 ± 0.16	22.93 ± 0.19	−1.35 ± 0.19		

[a] −, reduced level of TPP (100 nM) in the OBGM medium for *T. denticola*.

represents a reduced TPP level, and 50 μM represents an overabundance of TPP. The expression levels of $tbpA_{Td}$ under these three different conditions were measured by qRT-PCR. Compared to that with the reduced TPP level, the amount of $tbpA_{Td}$ transcript was decreased approximately 16-fold (ranging from 13- to 20-fold) in the presence of 10 μM TPP and 24-fold (ranging from 21- to 27-fold) in the presence of 50 μM TPP (Table 3). To further confirm the qRT-PCR results, Western blotting using a $TbpA_{Td}$ antiserum was conducted. Compared to that with the reduced TPP level, the level of $TbpA_{Td}$ was decreased 3.8-fold (10 μM) and 9.8-fold (50 μM), respectively (Fig. 6). The observed pattern is similar to that in the qRT-PCR analysis. Collectively, these results further confirm that $Td_{thi\text{-box}}$ is a TPP-sensing riboswitch that negatively controls the expression level of the $tbpABC_{Td}$ operon at the transcriptional level.

Isolation and characterization of the *T. denticola* Δ*tbpA* mutant. To further study the function of the $tbpABC_{Td}$ operon, the *TDE0143* gene was inactivated by targeted mutagenesis as illustrated in Fig. 1. Approximate 80 erythromycin-resistant (Erm^r) colonies appeared 10 days after the plating, and these colonies were first screened by PCR with primers specific to Erm^r. A total of 20 positive colonies were detected. One clone was further analyzed by PCR with different pairs of primers at the flanking region of *TDE0143*. The results showed that the target gene was deleted and replaced with the Erm^r cassette as expected (data not shown). Western blotting with a specific antibody to $TbpA_{Td}$ further showed that the cognate gene product was inactivated in the mutant (Fig. 7a). The obtained mutant was referred to as *T. denticola* Δ*tbpA*. Since the $tbpA_{Td}$ operon is polycistronic, the insertion of the Erm^r cassette in *TDE0143* may alter the expression of downstream genes and thus complicate subsequent interpretations. However, the RT-PCR analysis showed that the insertion of Erm^r did not have any impact on the expression of downstream genes *TDE0144* and *TDE0145* (Fig. 7b), which could rule out the existence of a polar effect in the *T. denticola* Δ*tbpA* mutant.

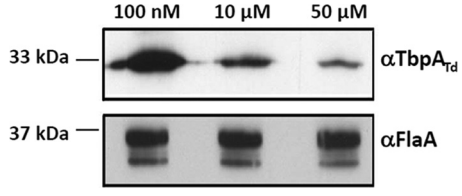

FIG. 6. The $TbpA_{Td}$ level is repressed by high concentrations of TPP. Wild-type *T. denticola* was cultivated in TA medium containing different concentrations of TPP (100 nM, 10 μM, and 50 μM), and the same amount of whole-cell lysates was analyzed by SDS-PAGE. Polyclonal antibodies against $TbpA_{Td}$ or FlaA, a flagellin protein of *T. denticola*, were used as probes. FlaA was used as an internal control.

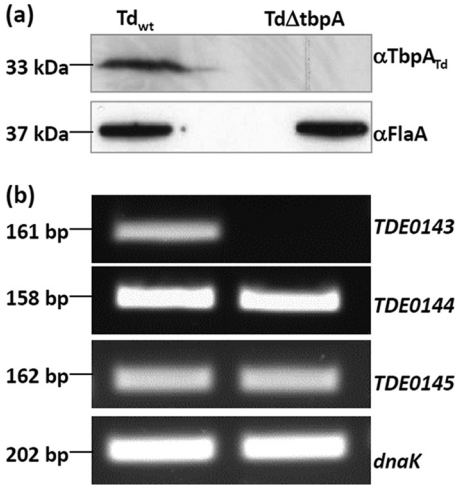

FIG. 7. Characterization of the *T. denticola* Δ*tbpA* mutant. (a) Western blotting of the *T. denticola* Δ*tbpA* mutant. The same amounts of wild-type *T. denticola* and *T. denticola* Δ*tbpA* whole lysates were analyzed by SDS-PAGE. The immunoblotting was conducted as described for Fig. 5b. (b) RT-PCR analysis of the *T. denticola* Δ*tbpA* mutant. The transcripts of *TDE0144* and *TDE0145*, the downstream genes of $tbpA_{Td}$, in wild-type *T. denticola* and *T. denticola* Δ*tbpA* were detected by RT-PCR.

$TbpA_{Td}$ is required for the growth of *T. denticola* when exogenous TPP is limited. *T. denticola* needs exogenous TPP to grow (16), and $TbpA_{Td}$ is a TPP-binding protein. Thus, we hypothesize that the inactivation of $tbpA_{Td}$ may influence the transport of exogenous TPP and the growth of the mutant. To test this hypothesis, the wild-type strain and the *T. denticola* Δ*tbpA* mutant were cultivated in TA medium with three different concentrations of TPP (100 nM, 10 μM, and 50 μM), and their growth curves were measured. As shown in Fig. 8, at the concentrations of 10 μM and 50 μM, the growth patterns of wild-type *T. denticola* and the *T. denticola* Δ*tbpA* mutant were almost identical. However, at the low TPP concentration (100 nM), the mutant failed to grow. In contrast, the wild-type strain had only a slightly decreased growth rate compared to those under the other two culture conditions (10 μM and 50 μM). These results demonstrate that $TbpA_{Td}$ is required for the growth of *T. denticola* when the exogenous TPP is limited.

Inactivation of $tbpA_{Td}$ represses the transport of exogenous TPP. TbpA is a TPP-binding protein (73, 80). To determine whether $TbpA_{Td}$ is involved in the transport of exogenous TPP, the intracellular level of TPP was measured by HPLC. As shown in Table 4, at the high TPP concentration (50 μM), the intracellular level of TPP in wild-type *T. denticola* (258.39 nM) was slightly higher than that in the mutant (230.34 nM). However, when the exogenous TPP was decreased (10 μM), the intracellular TPP level in the mutant (94.49 nM) was about 50% less than that in the wild-type strain (184.85 nM). These results show that the absence of $TbpA_{Td}$ significantly reduces the transport of exogenous TPP, suggesting that $TbpA_{Td}$ is required for the transport of TPP, in particular when the exogenous TPP is limited.

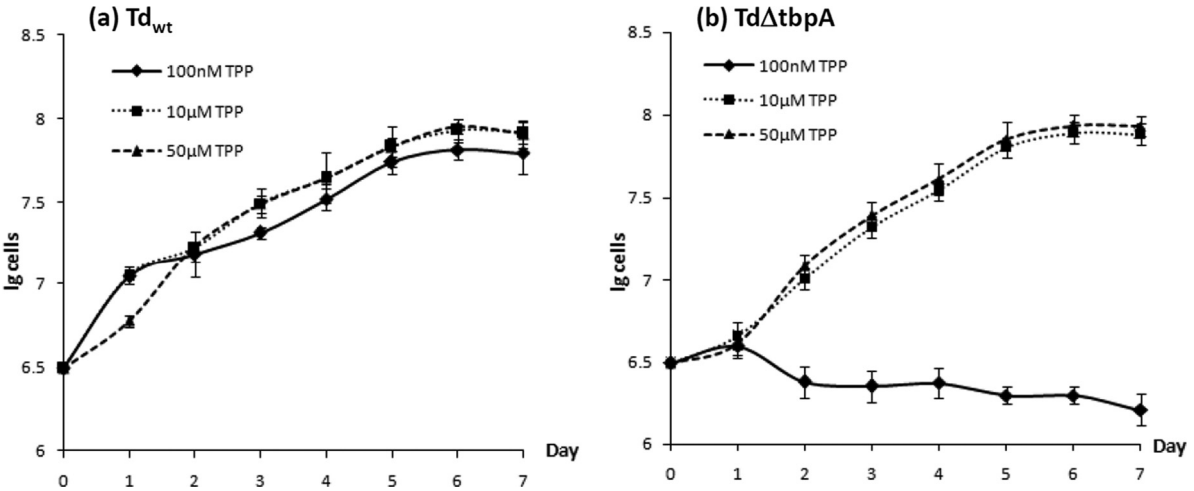

FIG. 8. Growth curves of wild-type *T. denticola* (a) and *T. denticola* Δ*tbpA* (b). The two strains were cultivated in TA medium containing three different concentrations of TPP (100 nM, 10 μM, and 50 μM). Cell counting was repeated in duplicate with at least three independent samples, and the results are expressed as mean ± SEM.

DISCUSSION

***T. denticola* lacks a *de novo* TPP biosynthesis pathway.** The *de novo* thiamine biosynthesis (TBS) pathway has been well studied in *E. coli* and *S.* Typhimurium, where it has been a model to understand TBS in other organisms (2, 34, 36). The synthesis of thiamine involves the separate formation of a thiazole moiety (THZ-P) and a pyrimidine moiety (HMP-P). HMP-P is typically synthesized by ThiC from an aminoimidazole ribotide that is derived from the purine biosynthesis pathway (10, 40). THZ-P is produced from pyruvate, tyrosine, and cysteine through a series of reactions that are catalyzed by several enzymes, such as ThiF, ThiS, ThiG, and ThiH (2, 34). The moieties of HMP-P and THZ-P are further condensed to TMP by ThiE (57, 78). However, all of these key enzymes are absent in the genome of *T. denticola* (70), suggesting that it lacks a *de novo* TBS pathway. Interestingly, a homolog of ThiD (TDE0693) is present in the genome of *T. denticola*. ThiD, a phosphomethyl pyrimidine kinase, converts HMP to HMP-P and then to HMP-PP (11). The function of this homolog is not clear. Given the absence of other key enzymes, it seems unlikely that TDE0693 is involved in *de novo* thiamine biosynthesis.

***T. denticola* lacks thiamine salvage biosynthesis pathways.** In addition to the *de novo* biosynthesis, a set of salvage pathways that utilize intermediate products or thiamine to synthesize TPP has been identified in different bacterial species (2, 34). In the enteric bacteria, thiazole alcohol can be converted to THZ-P by ThiM, a thiazole kinase. In *Bacillus subtilis*, HMP can be synthesized from formylaminopyrimidine, which is directly transported from the environment by the ThiXYZ transporter (32). However, genome mining analysis did not find any homologs of these salvage pathways in *T. denticola*. In addition, TPP can be directly derived from thiamine (49, 81). In the enteric bacteria, thiamine can be converted to TMP by ThiK (thiamine kinase) and then to TPP by ThiL. In *B. subtilis*, thiamine is directly converted to TPP by YloS, a thiamine pyrophosphokinase. However, none of these homologs were identified in the genome of *T. denticola*. To further determine whether *T. denticola* is able to directly use thiamine, the *T. denticola* Δ*tbpA* mutant was cultivated in TA medium containing different concentrations of thiamine (10 μM, 50 μM, and 100 μM). It was found that the mutant failed to grow in the presence of thiamine, suggesting that *T. denticola* is unable to produce TPP via the salvage pathway of metabolizing thiamine. Collectively, the above-described bioinformatic and genetic analyses have demonstrated that *T. denticola* lacks an endogenous TBS pathway, meaning that it has to utilize exogenous TPP.

TABLE 4. Comparison of intracellular TPP levels in wild-type *T. denticola* and the Δ*tbpA* mutant[a]

TPP concn in TA medium	Mean intracellular TPP concn (nM) ± SEM in:	
	Wild-type *T. denticola*	Δ*tbpA* mutant
100 nM	94.43 ± 8.96	
10 μM	184.85 ± 4.52	94.49 ± 6.97
50 μM	258.39 ± 7.21	230.34 ± 4.3

[a] The two strains were cultivated in TA medium containing different concentrations of TPP (100 nM, 10 μM, and 50 μM). Three independent assays were conducted, and the intracellular concentrations of TPP were determined. The Δ*tbpA* mutant failed to grow at the low concentration of TPP (100 nM).

Is TbpA$_{Td}$ the sole TPP transporter in *T. denticola*? Interestingly, when the exogenous TPP is sufficient, the *T. denticola* Δ*tbpA* mutant is still able to take up TPP. For example, in the presence of 50 μM TPP, the intracellular concentration of TPP in the mutant (230 nM) is only slightly lower than that in the wild type (258 nM), suggesting that the exogenous TPP is still able to enter into the mutant cells via certain mechanisms. A similar phenotype was observed in *S.* Typhimurium; a *thiP thiH* double mutant, in which both the *de novo* TBS pathway and the TPP transporter were blocked, failed to grow in a low concentration of TPP (100 nM) (80). The possible mechanism could be either that there is an additional unidentified TPP transporter that is independent of ThiBPQ or that the remaining part of the TPP ABC transporter (a permease and an ATPase) is still able to transport TPP. Several lines of evidence suggest

that the first possibility is unlikely. First, the thiamine-binding proteins are well conserved. Besides ThiB, no additional homolog has yet been identified in the enteric bacteria or *T. denticola*. Second, *T. denticola* lacks a ThiBPQ-independent thiamine transporter (e.g., the ThiXYZ transporter of *B. subtilis*) (32, 62). Finally, both *T. denticola* Δ*tbpA* and the *thiP thiH* double mutant fail to grow when the exogenous TPP is limited (80), suggesting that either no additional TPP transporter exists or if it exists, the transport efficiency of exogenous TPP is quite limited. As such, the second mechanism proposed above is more compelling. As a thiamine-binding protein, $TbpA_{Td}$ is probably able to concentrate TPP from the environment and facilitate the transport of TPP. In the absence of $TbpA_{Td}$, the remaining transporter (a permease and an ATPase) is still able to uptake exogenous TPP, but its transport efficiency is significantly decreased. Therefore, when the exogenous TPP is limited, the *T. denticola* Δ*tbpA* mutant is incapable of ensuring the minimal requirement of TPP, and thus the mutant fails to grow. This proposition was reinforced by our inability to inactivate either the *TDE0144* (encoding a permease) or the *TDE0145* (encoding an ATPase) gene.

$Td_{thi\text{-box}}$ primarily regulates the *$tbpABC_{Td}$* operon at the transcriptional level. The TPP-sensing riboswitches *thiC* and *thiM* are composed of five helices, three junction bulges, and two terminal loops (69, 82). In the presence of TPP, two of the junction bulges bind to the pyrimidine ring and the pyrophosphate of TPP, forming a stable aptamer (19, 50, 69, 76). The *thi*-box of *thiM* incorporates the S/D sequence. It represses gene expression at the translational level by sequestering the S/D sequence and preventing translation (54, 82). Similar to the case for *thiM*, the predicted $Td_{thi\text{-box}}$ incorporates the S/D sequence (Fig. 4). Therefore, it may regulate gene expression at the translational level, like its counterpart *thiM*. However, the qRT-PCR analysis showed that the addition of TPP significantly decreased the levels of *lacZ* and *$tbpA_{Td}$* transcripts (Tables 2 and 3). Such attenuations are proportional to the reduction of the β-galactosidase activity and $TbpA_{Td}$ protein, suggesting that the action of $Td_{thi\text{-box}}$ occurs primarily at the transcriptional level. $Td_{thi\text{-box}}$ partially overlaps the identified P_{tbpA} promoter (Fig. 4; see Fig. S2 in the supplemental material). It is most likely that in the presence of TPP, $Td_{thi\text{-box}}$ form a stable aptamer that acts as a transcription terminator and blocks transcription. As the S/D sequence is sequestered by the aptamer of $Td_{thi\text{-box}}$, it is also possible that the translational regulation makes some contribution to the function of $Td_{thi\text{-box}}$. At this point, the existence of this possibility cannot be completely ruled out.

The regulatory mechanism of TPP transport in *T. denticola*. Based on the results and the above discussions, a working model to illustrate the regulatory mechanism of TPP transport in *T. denticola* is proposed (Fig. 9). *T. denticola* lacks a *de novo* TBS pathway, and it depends on a TPP ABC transporter to take up exogenous TPP. The genes that encode this transport system form an operon (*$tbpABC_{Td}$*) that is regulated by a TPP-sensing riboswitch ($Td_{thi\text{-box}}$). When the exogenous TPP is limited and the intracellular TPP is insufficient, $Td_{thi\text{-box}}$ folds into a structure that allows the expression of the *$tbpABC_{Td}$* operon. As such, more TPP transporter will be synthesized to transport exogenous TPP into the cells. When the intracellular TPP becomes sufficient, the free TPP binds to the $Td_{thi\text{-box}}$ and forms a stable aptamer, which represses the transcription of the *$tbpABC_{Td}$* operon and limits the uptake of exogenous TPP. This feedback inhibition mechanism can allow the spirochete to maintain a constant intracellular level of TPP to meet its growth requirements in response to the varied environments in the oral flora.

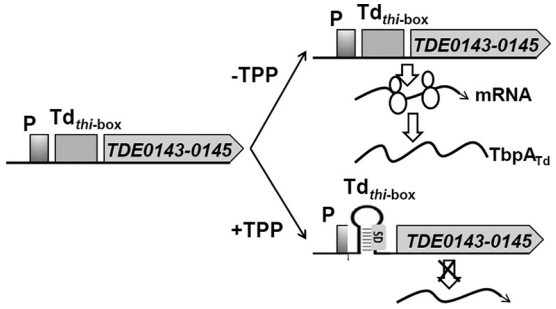

FIG. 9. Schematic diagram showing the regulatory mechanism of TPP transport in *T. denticola*. *T. denticola* lacks a *de novo* TBS pathway, and it depends on the TPP transporter to take up exogenous TPP. The *$tbpABC_{Td}$* operon encodes a TPP ABC transporter, which is regulated by a TPP-sensing riboswitch ($Td_{thi\text{-box}}$). When the intracellular TPP is insufficient, $Td_{thi\text{-box}}$ folds into a structure that allows the transcription of the *$tbpABC_{Td}$* operon, and more TPP transporter will be synthesized to take up exogenous TPP into the cells. When the intracellular TPP becomes sufficient, the free TPP binds to $Td_{thi\text{-box}}$ and forms a stable aptamer, which in turn represses the transcription of the *$tbpABC_{Td}$* operon and limits the uptake of exogenous TPP.

Thiamine metabolism in spirochetes. TPP is an essential cofactor for several important enzymes of carbohydrate metabolism (2). For example, TPP is a coenzyme of pyruvate dehydrogenase that converts pyruvate to acetyl coenzyme A (acetyl-CoA). Acetyl-CoA can be further metabolized to produce ATP via the tricarboxylic acid (TCA) cycle. In addition, thiamine biosynthesis is linked to other central metabolism pathways (e.g., purine biosynthesis) (36). Thus, thiamine biosynthesis has been used in systems biology to dissect metabolic integration in microorganisms. Spirochetes are a group of medically important but poorly understood bacteria (1, 9). Most spirochetes have fastidious growth requirements. To begin to understand thiamine metabolism in spirochetes, we searched the genomes of sequenced spirochetes, including *Borrelia* spp., *Brachyspira* spp., *Leptospira* spp., and *Treponema* spp. It was found that *Brachyspira* spp. (*B. hyodysenteriae* and *B. pilosicoli*) and *Leptospira* spp. (*L. biflexa*, *L. borgetersenii*, and *L. interrogans*) contain a *de novo* TBS pathway (3, 6, 58, 61, 79). Along with *T. denticola*, *T. pallidum* and *T. vincentii* also lack a *de novo* TBS pathway (25). Similarly to *T. denticola*, they all contain a conserved TPP ABC transporter. For example, the homolog of TbpA in *T. pallidum* (TP0144) has 39% identity and 59% similarity to $TbpA_{Td}$. Interestingly, neither the *de novo* TBS pathway nor the TPP ABC transporter has been found in any *Borrelia* sp. (24).

ACKNOWLEDGMENTS

We thank R. Limberger for providing *T. denticola* strains, R. Breaker for providing the pRS414 plasmid, and C. Fenno for providing the anti-FlaA serum.

This research was supported by Public Health Service grants DE019667 and AI078958 to C. Li.

REFERENCES

1. **Baranton, G., and I. G. Old.** 1995. The spirochetes: a different way of life. Bull. Inst. Pasteur **93:**63–95.
2. **Begley, T. P., et al.** 1999. Thiamin biosynthesis in prokaryotes. Arch. Microbiol. **171:**293–300.
3. **Bellgard, M. I., et al.** 2009. Genome sequence of the pathogenic intestinal spirochete *Brachyspira hyodysenteriae* reveals adaptations to its lifestyle in the porcine large intestine. PLoS One **4:**e4641.
4. **Blakemore, R. P., and E. Canale-Parola.** 1976. Arginine catabolism by *Treponema denticola*. J. Bacteriol. **128:**616–622.
5. **Breaker, R. R.** 2008. Complex riboswitches. Science **319:**1795–1797.
6. **Bulach, D. M., et al.** 2006. Genome reduction in *Leptospira borgpetersenii* reflects limited transmission potential. Proc. Natl. Acad. Sci. U. S. A. **103:** 14560–14565.
7. **Capone, R. F., Y. Ning, N. Pakulis, T. Alhazzazi, and J. C. Fenno.** 2007. Characterization of *Treponema denticola pyrF* encoding orotidine-5′-monophosphate decarboxylase. FEMS Microbiol. Lett. **268:**261–267.
8. **Chan, E. C., and R. McLaughlin.** 2000. Taxonomy and virulence of oral spirochetes. Oral Microbiol. Immunol. **15:**1–9.
9. **Charon, N. W., and S. F. Goldstein.** 2002. Genetics of motility and chemotaxis of a fascinating group of bacteria: the spirochetes. Annu. Rev. Genet. **36:**47–73.
10. **Chatterjee, A., et al.** 2008. Reconstitution of ThiC in thiamine pyrimidine biosynthesis expands the radical SAM superfamily. Nat. Chem. Biol. **4:**758–765.
11. **Cheng, G., E. M. Bennett, T. P. Begley, and S. E. Ealick.** 2002. Crystal structure of 4-amino-5-hydroxymethyl-2-methylpyrimidine phosphate kinase from Salmonella typhimurium at 2.3 A resolution. Structure **10:**225–235.
12. **Clark, D. T., and M. Soory.** 2006. The metabolism of cholesterol and certain hormonal steroids by *Treponema denticola*. Steroids **71:**352–363.
13. **Darveau, R. P.** 2010. Periodontitis: a polymicrobial disruption of host homeostasis. Nat. Rev. Microbiol. **8:**481–490.
14. **Dashper, S. G., C. A. Seers, K. H. Tan, and E. C. Reynolds.** 2010. Virulence factors of the oral spirochete *Treponema denticola.* J. Dent. Res. doi: 0022034510385242.
15. **Davidson, A. L., and J. Chen.** 2004. ATP-binding cassette transporters in bacteria. Annu. Rev. Biochem. **73:**241–268.
16. **De Ciccio, A., R. McLaughlin, and E. C. Chan.** 1999. Factors affecting the formation of spherical bodies in the spirochete *Treponema denticola*. Oral Microbiol. Immunol. **14:**384–386.
17. **Dewhirst, F. E., et al.** 2000. The diversity of periodontal spirochetes by 16S rRNA analysis. Oral Microbiol. Immunol. **15:**196–202.
18. **Downs, D. M.** 2006. Understanding microbial metabolism. Annu. Rev. Microbiol. **60:**533–559.
19. **Edwards, T. E., and A. R. Ferre-D'Amare.** 2006. Crystal structures of the thi-box riboswitch bound to thiamine pyrophosphate analogs reveal adaptive RNA-small molecule recognition. Structure **14:**1459–1468.
20. **Ellen, R. P., and V. B. Galimanas.** 2005. Spirochetes at the forefront of periodontal infections. Periodontology 2000 **38:**13–32.
21. **Fenno, J. C., and B. C. McBride.** 1998. Virulence factors of oral treponemes. Anaerobe **4:**1–17.
22. **Fenno, J. C., et al.** 2000. Identification of a *Treponema denticola* OppA homologue that binds host proteins present in the subgingival environment. Infect. Immun. **68:**1884–1892.
23. **Finn, R. D., et al.** 2010. The Pfam protein families database. Nucleic Acids Res. **38:**D211–D222.
24. **Fraser, C. M., et al.** 1997. Genomic sequence of a Lyme disease spirochaete, *Borrelia burgdorferi*. Nature **390:**580–586.
25. **Fraser, C. M., et al.** 1998. Complete genome sequence of *Treponema pallidum*, the syphilis spirochete. Science **281:**375–388.
26. **Gaal, T., et al.** 2001. Promoter recognition and discrimination by EsigmaS RNA polymerase. Mol. Microbiol. **42:**939–954.
27. **Gardner, P. P., et al.** 2009. Rfam: updates to the RNA families database. Nucleic Acids Res. **37:**D136–D140.
28. **Haffajee, A. D., and S. S. Socransky.** 2005. Microbiology of periodontal diseases: introduction. Periodontology 2000 **38:**9–12.
29. **Hespell, R. B., and E. Canale-Parola.** 1971. Amino acid and glucose fermentation by *Treponema denticola*. Arch. Mikrobiol. **78:**234–251.
30. **Holt, S. C., and J. L. Ebersole.** 2005. *Porphyromonas gingivalis*, *Treponema denticola*, and *Tannerella forsythia*: the "red complex," a prototype polybacterial pathogenic consortium in periodontitis. Periodontology 2000 **38:**72–122.
31. **Jackson-Rosario, S., and W. T. Self.** 2009. Inhibition of selenium metabolism in the oral pathogen *Treponema denticola*. J. Bacteriol. **191:**4035–4040.
32. **Jenkins, A. H., G. Schyns, S. Potot, G. Sun, and T. P. Begley.** 2007. A new thiamin salvage pathway. Nat. Chem. Biol. **3:**492–497.
33. **Jones, P. M., and A. M. George.** 2004. The ABC transporter structure and mechanism: perspectives on recent research. Cell Mol. Life Sci. **61:**682–699.
34. **Jurgenson, C. T., T. P. Begley, and S. E. Ealick.** 2009. The structural and biochemical foundations of thiamin biosynthesis. Annu. Rev. Biochem. **78:** 569–603.
35. **Kent, C., P. Gee, S. Y. Lee, X. Bian, and J. C. Fenno.** 2004. A CDP-choline pathway for phosphatidylcholine biosynthesis in *Treponema denticola*. Mol. Microbiol. **51:**471–481.
36. **Koenigsknecht, M. J., and D. M. Downs.** 2010. Thiamine biosynthesis can be used to dissect metabolic integration. Trends Microbiol. **18:**240–247.
37. **Korner, R. W., A. Vierzig, B. Roth, and C. Muller.** 2009. Determination of thiamin diphosphate in whole blood samples by high-performance liquid chromatography—a method suitable for pediatric diagnostics. J. Chromatogr. B Anal. Technol. Biomed. Life Sci. **877:**1882–1886.
38. **Kulshina, N., T. E. Edwards, and A. R. Ferre-D'Amare.** 2010. Thermodynamic analysis of ligand binding and ligand binding-induced tertiary structure formation by the thiamine pyrophosphate riboswitch. RNA **16:**186–196.
39. **Kuramitsu, H. K.** 2003. Molecular genetic analysis of the virulence of oral bacterial pathogens: an historical perspective. Crit. Rev. Oral Biol. Med. **14:**331–344.
40. **Lawhorn, B. G., R. A. Mehl, and T. P. Begley.** 2004. Biosynthesis of the thiamin pyrimidine: the reconstitution of a remarkable rearrangement reaction. Org. Biomol. Chem. **2:**2538–2546.
41. **Lepp, P. W., et al.** 2004. Methanogenic archaea and human periodontal disease. Proc. Natl. Acad. Sci. U. S. A. **101:**6176–6181.
42. **Li, C., M. Sal, M. Marko, and N. W. Charon.** 2010. Differential regulation of the multiple flagellins in spirochetes. J. Bacteriol. **192:**2596–2603.
43. **Li, C., H. Xu, K. Zhang, and F. T. Liang.** 2010. Inactivation of a putative flagellar motor switch protein FliG1 prevents *Borrelia burgdorferi* from swimming in highly viscous media and blocks its infectivity. Mol. Microbiol. **75:**1563–1576.
44. **Li, H., J. Ruby, N. Charon, and H. Kuramitsu.** 1996. Gene inactivation in the oral spirochete *Treponema denticola*: construction of an *flgE* mutant. J. Bacteriol. **178:**3664–3667.
45. **Limberger, R. J., L. L. Slivienski, J. Izard, and W. A. Samsonoff.** 1999. Insertional inactivation of *Treponema denticola tap1* results in a nonmotile mutant with elongated flagellar hooks. J. Bacteriol. **181:**3743–3750.
46. **Loesche, W. J.** 1988. The role of spirochetes in periodontal disease. Adv. Dent. Res. **2:**275–283.
47. **Lu, J., and E. L. Frank.** 2008. Rapid HPLC measurement of thiamine and its phosphate esters in whole blood. Clin. Chem. **54:**901–906.
48. **Marchler-Bauer, A., et al.** 2009. CDD: specific functional annotation with the Conserved Domain Database. Nucleic Acids Res. **37:**D205–D210.
49. **Melnick, J., et al.** 2004. Identification of the two missing bacterial genes involved in thiamine salvage: thiamine pyrophosphokinase and thiamine kinase. J. Bacteriol. **186:**3660–3662.
50. **Miranda-Rios, J.** 2007. The THI-box riboswitch, or how RNA binds thiamin pyrophosphate. Structure **15:**259–265.
51. **Miranda-Rios, J., M. Navarro, and M. Soberon.** 2001. A conserved RNA structure (thi box) is involved in regulation of thiamin biosynthetic gene expression in bacteria. Proc. Natl. Acad. Sci. U. S. A. **98:**9736–9741.
52. **Mironov, A. S., et al.** 2002. Sensing small molecules by nascent RNA: a mechanism to control transcription in bacteria. Cell **111:**747–756.
53. **Nudler, E., and A. S. Mironov.** 2004. The riboswitch control of bacterial metabolism. Trends Biochem. Sci. **29:**11–17.
54. **Ontiveros-Palacios, N., et al.** 2008. Molecular basis of gene regulation by the THI-box riboswitch. Mol. Microbiol. **67:**793–803.
55. **Orth, R., N. O'Brien-Simpson, S. Dashper, K. Walsh, and E. Reynolds.** 2010. An efficient method for enumerating oral spirochetes using flow cytometry. J. Microbiol. Methods **80:**123–128.
56. **Paster, B. J., et al.** 2001. Bacterial diversity in human subgingival plaque. J. Bacteriol. **183:**3770–3783.
57. **Peapus, D. H., et al.** 2001. Structural characterization of the enzyme-substrate, enzyme-intermediate, and enzyme-product complexes of thiamin phosphate synthase. Biochemistry **40:**10103–10114.
58. **Picardeau, M., et al.** 2008. Genome sequence of the saprophyte *Leptospira biflexa* provides insights into the evolution of *Leptospira* and the pathogenesis of leptospirosis. PLoS One **3:**e1607.
59. **Pihlstrom, B. L., B. S. Michalowicz, and N. W. Johnson.** 2005. Periodontal diseases. Lancet **366:**1809–1820.
60. **Regulski, E. E., et al.** 2008. A widespread riboswitch candidate that controls bacterial genes involved in molybdenum cofactor and tungsten cofactor metabolism. Mol. Microbiol. **68:**918–932.
61. **Ren, S. X., et al.** 2003. Unique physiological and pathogenic features of *Leptospira interrogans* revealed by whole-genome sequencing. Nature **422:** 888–893.
62. **Rodionov, D. A., A. G. Vitreschak, A. A. Mironov, and M. S. Gelfand.** 2002. Comparative genomics of thiamin biosynthesis in procaryotes. New genes and regulatory mechanisms. J. Biol. Chem. **277:**48949–48959.
63. **Rother, M., A. Bock, and C. Wyss.** 2001. Selenium-dependent growth of *Treponema denticola*: evidence for a clostridial-type glycine reductase. Arch. Microbiol. **177:**113–116.
64. **Ruby, J. D., et al.** 1997. Relationship of *Treponema denticola* periplasmic flagella to irregular cell morphology. J. Bacteriol. **179:**1628–1635.
65. **Sal, M. S., et al.** 2008. *Borrelia burgdorferi* uniquely regulates its motility genes and has an intricate flagellar hook-basal body structure. J. Bacteriol. **190:**1912–1921.

66. **Sali, A., and T. L. Blundell.** 1993. Comparative protein modelling by satisfaction of spatial restraints. J. Mol. Biol. **234:**779–815.
67. **Sela, M. N.** 2001. Role of *Treponema denticola* in periodontal diseases. Crit. Rev. Oral Biol. Med. **12:**399–413.
68. **Serganov, A., and D. J. Patel.** 2007. Ribozymes, riboswitches and beyond: regulation of gene expression without proteins. Nat. Rev. Genet. **8:**776–790.
69. **Serganov, A., A. Polonskaia, A. T. Phan, R. R. Breaker, and D. J. Patel.** 2006. Structural basis for gene regulation by a thiamine pyrophosphate-sensing riboswitch. Nature **441:**1167–1171.
70. **Seshadri, R., et al.** 2004. Comparison of the genome of the oral pathogen *Treponema denticola* with other spirochete genomes. Proc. Natl. Acad. Sci. U. S. A. **101:**5646–5651.
71. **Simons, R. W., F. Houman, and N. Kleckner.** 1987. Improved single and multicopy lac-based cloning vectors for protein and operon fusions. Gene **53:**85–96.
72. **Socransky, S. S., and A. D. Haffajee.** 2005. Periodontal microbial ecology. Periodontology 2000 **38:**135–187.
73. **Soriano, E. V., et al.** 2008. Structural similarities between thiamin-binding protein and thiaminase-I suggest a common ancestor. Biochemistry **47:**1346–1357.
74. **Sze, C. W., and C. Li.** 2011. Inactivation of bb0184, which encodes carbon storage regulator A, represses the infectivity of *Borrelia burgdorferi*. Infect. Immun. **79:**1270–1279.
75. **Tatakis, D. N., and P. S. Kumar.** 2005. Etiology and pathogenesis of periodontal diseases. Dent. Clin. North Am. **49:**491–516.
76. **Thore, S., M. Leibundgut, and N. Ban.** 2006. Structure of the eukaryotic thiamine pyrophosphate riboswitch with its regulatory ligand. Science **312:**1208–1211.
77. **Typas, A., S. Stella, R. C. Johnson, and R. Hengge.** 2007. The −35 sequence location and the Fis-sigma factor interface determine sigmas selectivity of the proP (P2) promoter in *Escherichia coli*. Mol. Microbiol. **63:**780–796.
78. **Vander Horn, P. B., A. D. Backstrom, V. Stewart, and T. P. Begley.** 1993. Structural genes for thiamine biosynthetic enzymes (thiCEFGH) in *Escherichia coli* K-12. J. Bacteriol. **175:**982–992.
79. **Wanchanthuek, P., et al.** 2010. The complete genome sequence of the pathogenic intestinal spirochete *Brachyspira pilosicoli* and comparison with other *Brachyspira* genomes. PLoS One **5:**e11455.
80. **Webb, E., K. Claas, and D. Downs.** 1998. *thiBPQ* encodes an ABC transporter required for transport of thiamine and thiamine pyrophosphate in *Salmonella typhimurium*. J. Biol. Chem. **273:**8946–8950.
81. **Webb, E., and D. Downs.** 1997. Characterization of *thiL*, encoding thiamin-monophosphate kinase, in *Salmonella typhimurium*. J. Biol. Chem. **272:**15702–15707.
82. **Winkler, W., A. Nahvi, and R. R. Breaker.** 2002. Thiamine derivatives bind messenger RNAs directly to regulate bacterial gene expression. Nature **419:**952–956.
83. **Winkler, W. C., and R. R. Breaker.** 2005. Regulation of bacterial gene expression by riboswitches. Annu. Rev. Microbiol. **59:**487–517.
84. **Yang, Y., and C. Li.** 2009. Transcription and genetic analyses of a putative N-acetylmuramyl-L-alanine amidase in *Borrelia burgdorferi*. FEMS Microbiol. Lett. **290:**164–173.
85. **Yang, Y., P. E. Stewart, X. Shi, and C. Li.** 2008. Development of a transposon mutagenesis system in the oral spirochete *Treponema denticola*. Appl. Environ. Microbiol. **74:**6461–6464.